Photosynthesis Research
https://doi.org/10.1007/s11120-020-00716-z

TECHNICAL COMMUNICATION

Using photorespiratory oxygen response to analyse leaf mesophyll resistance

Xinyou Yin[1] · Peter E. L. van der Putten[1] · Daniel Belay[2] · Paul C. Struik[1]

Received: 27 November 2019 / Accepted: 27 January 2020

Abstract

Classical approaches to estimate mesophyll conductance ignore differences in resistance components for CO_2 from intercellular air spaces (IAS) and CO_2 from photorespiration (F) and respiration (R_d). Consequently, mesophyll conductance apparently becomes sensitive to (photo)respiration relative to net photosynthesis, $(F+R_d)/A$. This sensitivity depends on several hard-to-measure anatomical properties of mesophyll cells. We developed a method to estimate the parameter m ($0 \le m \le 1$) that lumps these anatomical properties, using gas exchange and chlorophyll fluorescence measurements where $(F+R_d)/A$ ratios vary. This method was applied to tomato and rice leaves measured at five O_2 levels. The estimated m was 0.3 for tomato but 0.0 for rice, suggesting that classical approaches implying $m=0$ work well for rice. The mesophyll conductance taking the m factor into account still responded to irradiance, CO_2, and O_2 levels, similar to response patterns of stomatal conductance to these variables. Largely due to different m values, the fraction of (photo)respired CO_2 being refixed within mesophyll cells was lower in tomato than in rice. But that was compensated for by the higher fraction via IAS, making the total re-fixation similar for both species. These results, agreeing with CO_2 compensation point estimates, support our method of effectively analysing mesophyll resistance.

Keywords CO_2 compensation point · CO_2 transfer · Internal conductance · O_2 response · Resistance · Re-assimilation

Introduction

Quantifying the CO_2 diffusion inside leaves of C_3 plants is important in both physiological and ecological contexts. Physiologists assess leaf photosynthetic efficiency and capacity, and both of them depend on how CO_2 from the atmosphere travel to the chloroplast stroma and how much CO_2 released by respiration and photorespiration ["(photo) respired CO_2" hereafter] can be refixed by Rubisco (Busch et al. 2013; von Caemmerer 2013). Ecologists often project the impact of global land CO_2 fertilization (Sun et al. 2014). The model of Farquhar, von Caemmerer and Berry (1980; "the FvCB model" hereafter), which is widely used as a component for this projection, requires the CO_2 level at carboxylation sites of Rubisco (C_c) as its input. The drawdown of C_c, relative to the CO_2 level in the ambient air (C_a), depends not only on stomatal conductance for CO_2 transfer (g_{sc}) but also on mesophyll conductance (g_m), such that (von Caemmerer and Evans 1991):

$$C_c = C_i - A/g_m \quad (1)$$

where C_i is the intercellular air space (IAS) CO_2 level and A is the net photosynthesis rate.

The FvCB model calculates A as the minimum of the Rubisco activity limited rate (A_c) and electron transport-limited rate (A_j) of photosynthesis, and Sharkey (1985) added a third limitation, accounting for the rate set by triose phosphate utilization (A_p) (see Supplementary Text S1). Equation (1) has been combined with the FvCB model to estimate g_m from combined data of gas exchange and chlorophyll fluorescence measurements on photosystem II (PSII) electron transport efficiency Φ_2 (Harley et al. 1992; Yin and Struik 2009). The most commonly used method to estimate g_m is

Electronic supplementary material The online version of this article (https://doi.org/10.1007/s11120-020-00716-z) contains supplementary material, which is available to authorized users.

✉ Xinyou Yin
Xinyou.yin@wur.nl

[1] Centre for Crop Systems Analysis, Wageningen University & Research, P.O. Box 430, 6700 AK Wageningen, The Netherlands

[2] Selale University, P.O. Box 245, Fiche, Ethiopia

Published online: 10 February 2020

the 'variable J method' (Harley et al. 1992), derived from the A_j part of the FvCB model, using measurements that have to include photorespiratory conditions (Laisk et al. 2006; see Supplementary Text S2). Equation (1) has also been used to estimate g_m from online carbon isotope discrimination measurements (e.g. Evans et al. 1994; Tazoe et al. 2011; Barbour et al. 2016a) or oxygen isotope techniques (Barbour et al. 2016b).

Equation (1), as the classical g_m model, treats the (photo) respired CO_2 in the same way as it treats the CO_2 flux that comes from the IAS. Mesophyll resistance (the inverse of mesophyll conductance) consists of components imposed by IAS, cell wall, plasmalemma, cytosol, chloroplast envelope and stroma (Evans et al. 2009; Terashima et al. 2011). Unlike the CO_2 from the IAS, the (photo)respired CO_2, mainly coming from the mitochondria, does not need to cross the cell wall and plasmalemma, and thus experiences a different resistance. For this reason, Tholen et al. (2012) developed an Equation for the drawdown of C_c, relative to C_i:

$$C_c = C_i - A\left(r_{wp} + r_{ch}\right) - (F + R_d)r_{ch} \tag{2}$$

where F and R_d are CO_2 fluxes from photorespiration and respiration, respectively, r_{wp} is the combined cell wall and plasma membrane resistance, and r_{ch} is the chloroplast envelope and stroma resistance (r_{ch}). Combining Eqs. (1) and (2) results in $g_m = 1/[r_{wp} + r_{ch} + r_{ch}(F + R_d)/A]$. Tholen et al. (2012) concluded that mesophyll conductance, as defined by Eq. (1), is influenced by the ratio of (photo)respired CO_2 release to net CO_2 uptake, $(F + R_d)/A$, thereby resulting in an apparent sensitivity of mesophyll conductance to $[CO_2]$ and $[O_2]$. As this sensitivity does not imply a change in intrinsic diffusion properties, g_m as defined by Eq. (1) is an apparent parameter. We shall call it the apparent mesophyll conductance ($g_{m,app}$). In developing their model, Tholen et al. (2012) assumed a negligible IAS and cytosol resistance, but Eq. (2) still holds if the IAS resistance is lumped into r_{wp}, and part of cytosol resistance is lumped into r_{wp}, and the remaining part is lumped into r_{ch} (Berghuijs et al. 2015). If r_{wp} and r_{ch} both represent physical resistances, the total mesophyll diffusion resistance ($r_{m,dif}$) is $r_{wp} + r_{ch}$, and the model of Tholen et al. can be rewritten as

$$g_{m,app} = \frac{1}{r_{m,dif}[1 + \omega(F + R_d)/A]} \tag{2a}$$

where ω is the fraction of r_{ch} in $r_{m,dif}$.

However, the relative position of mitochondria and chloroplasts is underrepresented in the model of Tholen et al. (2012). Considering six scenarios of the arrangement of these organelles, Yin and Struik (2017) derived the model: $g_{m,app} = 1/\{r_{m,dif}[1 + \omega(1 - \lambda k)(F + R_d)/A]\}$, where λ is the fraction of mitochondria located in the inner cytosol (i.e. the cytosol area between chloroplasts and vacuole), and k is a factor allowing an increase ($k > 1$), no change ($k = 1$), and a decrease ($0 \le k < 1$) in the fraction of inner (photo)respired CO_2, caused by gaps when chloroplasts are not continuously aligned. The gaps largely depend on the anatomical parameter S_c/S_m, the ratio of chloroplast area to the mesophyll area exposed to IAS (Sage and Sage 2009). As $(1 - \lambda k)$ is between 0 and 1, the model predicts that the sensitivity of $g_{m,app}$ to $(F + R_d)/A$ is lower than Tholen et al. (2012) initially stated (Yin and Struik 2017). The model of Tholen et al. applies to an extreme case, either where mitochondria are located exclusively in the outer cytosol between plasmalemma and chloroplasts ($\lambda = 0$) or where (photo)respired CO_2 are completely mixed in cytosol if cytosol resistance is negligible and there are chloroplast gaps ($k \to 0$). In another extreme case where mitochondria are located exclusively in the inner cytosol ($\lambda = 1$) and chloroplasts cover completely the cell periphery ($k = 1$), the model predicts no sensitivity of $g_{m,app}$ to $(F + R_d)/A$, and Eq. (1) would work well as $g_{m,app}$ becomes $g_{m,dif}$ ($= 1/r_{m,dif}$). Equation (1) also works when r_{ch} is negligible compared to r_{wp} ($\omega = 0$) as if (photo) respired CO_2 is released in the same organelle where RuBP carboxylation occurs. Either situation ($\lambda k = 1$ or $\omega = 0$) can be approximately represented by leaves where mitochondria lies only in the inner cytosol, intimately behind chloroplasts that form a continuum.

Most likely scenarios are somewhere between the two extremes defined by Eqs. (1) and (2), that is, $0 < \lambda k < 1$ and $0 < \omega < 1$. All these scenarios result in different fractions of re-assimilation of (photo)respired CO_2 (Yin and Struik 2017), both within mesophyll cells and via IAS (see Supplementary Text S3). It would be useful if ω, λ and k can be measured. One way to derive ω is to use individual resistances that can be calculated from microscopic measurements on leaf anatomy (Evans et al. 1994; Peguero-Pino et al. 2012; Tosen et al. 2012a, b; Tomas et al. 2013; Berghuijs et al. 2015), despite uncertainties in the value of gas diffusion coefficients. Another possible method to estimate ω is to first estimate r_{wp} from oxygen isotope techniques assuming that the outer limit of carbonic anhydrase activity represents the cytosol immediately adjacent to the cell wall (Barbour 2017). Parameter λ can be assessed using electron microscope images for mitochondria distribution (Hatakeyama and Ueno 2016). Most difficult is to measure k, which depends on S_c/S_m. However, whether a high S_c/S_m would make $k > 1$ or < 1 would depend on the λ value as well as on cytosol resistance, and such a complex relationship is hard to quantify with a simple resistance model. However, because ω, λ and k lump together co-defining the sensitivity of $g_{m,app}$ to $(F + R_d)/A$, the model of Yin and Struik (2017) can be rewritten to

$$g_{m,app} = \frac{1}{r_{m,dif}[1 + m(F + R_d)/A]} \quad (3)$$

where $m = \omega\ (1 - \lambda k)$. Although Eq. (3) looks the same as Eq. (2a), their underlying intracellular fluxes for CO_2 gradient and re-assimilation differ (see Supplementary Text S3). Equation (3) may be used for estimating m from noninvasive gas exchange measurements where $(F + R_d)/A$ varies.

Many reports (e.g. Flexas et al. 2007a; Vrábl et al. 2009; Yin et al. 2009; Tazoe et al. 2011) showed that $g_{m,app}$ responds to changes in $[CO_2]$ or irradiance levels. $g_{m,app}$ was shown in tobacco to increase when $[O_2]$ was decreased from 21 to 1% (Tholen et al. 2012). All these responses can be described using a phenomenological equation (Yin et al. 2009). Tholen et al. (2012) explained the O_2 response and the commonly observed decline of $g_{m,app}$ with decreasing CO_2 below the ambient level (e.g. Flexas et al. 2007a; Vrábl et al. 2009; Yin et al. 2009), based on the earlier introduced sensitivity of $g_{m,app}$ to $(F + R_d)/A$, because both increasing O_2 and decreasing C_i increase $(F + R_d)/A$. However, the sensitivity of $g_{m,app}$ to $(F + R_d)/A$ cannot explain the observed response of $g_{m,app}$ to irradiances. Moreover, it is unknown whether $g_{m,dif}$ would be conserved across irradiance, CO_2 and O_2 levels.

In this study, we described a method that explores varying $(F + R_d)/A$ ratios to analyse mesophyll resistance from combined gas exchange and chlorophyll fluorescence measurements. The varying $(F + R_d)/A$ ratios were mainly created using five levels of O_2, on two contrasting species tomato and rice. Using these data, we assessed (i) the value of the m factor and whether it differs between species, (ii) whether $g_{m,dif}$ responds to $[CO_2]$, irradiance and $[O_2]$, and (iii) how the re-assimilation of (photo)respired CO_2 is affected by the m factor.

Materials and methods

Experiments and growth conditions

Seeds of tomato and rice were sown, and uniform seedlings were transplanted into pots 2 weeks after sowing, in glasshouse compartments. Pots were filled with soil, and after assessing initial soil nutrient contents, extra nutrients were applied (Table 1). Tomato plants were watered regularly, while rice plants were maintained submerged.

About 60% of the radiation incident on the glasshouse was transmitted to the plant level. During daytime supplemental light from 600 W HPS Hortilux Schréder lamps

Table 1 Growth and measurement conditions during the experiments with tomato and rice

	Tomato (cv. Growdena)	Rice (cv. IR64)
Growth condition		
Pot size and soil	10 L, with potting soil	7 L, with sandy soil
Initial nutrients (pot^{-1})	1.0 g N, 1.2 g P_2O_5, and 2.1 g K_2O	0.40 g N
Total additional nutrients (pot^{-1})	0.38 g N, 0.12 g P_2O_5, and 0.40 g K_2O	0.50 g N, 0.50 g P_2O_5 and 0.50 g K_2O
Temperature (day/night, °C)	21.4/17.0	28/23
Relative humidity (%)	ca 65	ca 65
Photoperiod (h d^{-1})	16	12
Supplementary lights on (W m^{-2}) [a]	≤150	≤400
Supplementary lights off (W m^{-2}) [b]	≥250	≥500
Measurement conditions		
Position of measured leaves (from the bottom)	the 9th layer leaf	the 9th main-culm leaf
$A - I_{inc}$ curves	I_{inc} = 20, 45, 70, 100, 150, 200, 500, 1000, 1500 µmol m^{-2} s^{-1} with C_a = 380 µmol mol^{-1} at each of O_2 levels 2%, 10%, 21%, 35% and 50%, or with C_a = 1000 µmol mol^{-1} and O_2 = 2%	I_{inc} = 45, 70, 100, 150, 200, 500, 1000, 1500 µmol m^{-2} s^{-1} with C_a = 380 µmol mol^{-1} at each of O_2 levels 2%, 10%, 21%, 35% and 50%, or with C_a = 1000 µmol mol^{-1} and O_2 = 2%
$A - C_i$ curves	C_a = 50, 65, 80, 100, 150, 200, 380, 760, 1000, 1500 µmol mol^{-1} with I_{inc} = 1000 µmol m^{-2} s^{-1} at each of O_2 levels 2%, 10%, 21%, 35% and 50%	C_a = 50, 65, 80, 100, 150, 200, 380, 600, 1000, 1500 µmol mol^{-1} with I_{inc} = 1000 µmol m^{-2} s^{-1} at each of O_2 levels 2%, 10%, 21%, 35% and 50%
Leaf temperature (°C)	25	25
Leaf-to-air vapour pressure difference (kPa)	0.7–1.5	0.7–1.5

[a]Threshold solar incident light outside glasshouse when supplementary lights were switched on;

[b]Threshold solar incident light outside glasshouse when supplementary lights were switched off

(Monster, NL) was automatically switched on when the incident solar flux dropped below a threshold and off when it exceeded a threshold outside glasshouse. These threshold levels were set different for tomato and rice (Table 1), to mimic growth environments of the two species.

Simultaneous gas exchange and chlorophyll fluorescence measurements

We used the Li-Cor-6400XT open gas exchange system with an integrated fluorescence head enclosing a 2-cm^2 area (Li-Cor Inc, Lincoln-NE, USA). Young but fully expanded leaves of four replicated plants from staggered sowings were measured for incident irradiance (I_{inc}) and C_a response curves in each species (Table 1).

Curves were measured at five O_2 concentrations (Table 1). Additional light response curves were obtained at 1000 µmol mol^{-1} C_a and 2% O_2 to establish nearly nonphotorespiratory conditions for calibration (see later). Gas from a cylinder containing a mixture of O_2 and N_2 was humidified and supplied via an overflow tube to the air inlet of the Li-Cor where CO_2 was blended with the gas, and the IRGA was adjusted for O_2 composition of the gas mixture according to the manufacturer's instructions. Based on pre-test measurements, we used 7–8 min for each step of an $A-I_{inc}$ curve, and 3–4 min for each step of an $A-C_i$ curve, to reach a steady state. All CO_2 exchange data were corrected for CO_2 leakage into and out of the leaf cuvette, using measurements on boiled leaves (Flexas et al. 2007b), and then C_i was re-calculated.

When A reached steady state at each light or CO_2 step, steady-state fluorescence (F_s) was recorded. Maximum fluorescence (F'_m) was measured using a 0.8 s light pulse of > 8000 µmol m^{-2} s^{-1}, or the multiphase flash with each phase of 300 ms and ramp depth of 40% (Loriaux et al. 2013). The PSII operating efficiency ($\Delta F/F'_m$) was set as $(F'_m - F_s)/F'_m$ (Genty et al. 1989).

Calibration and pre-determination of R_d and Rubisco parameters

Setting that $\Phi_2 = \Delta F/F'_m$, R_d was estimated as the negative intercept of a linear regression of A against ($I_{inc}\Phi_2/4$) using data of $A-I_{inc}$ curves within the electron transport-limited range for the nonphotorespiratory condition (Yin et al. 2009, 2011). The slope of the regression yields a calibration factor (s), which lumps (1) absorptance by leaf photosynthetic pigments, (2) the factor for excitation partitioning to PSII, (3) basal forms of alternative electron transport, (4) any difference between real efficiency of PSII electron transport (Φ_2) and $\Delta F/F'_m$, and (5) possibly difference in chloroplast populations sampled by gas exchange and by chlorophyll fluorescence (van der Putten et al. 2018). The electron transport rate J can then be obtained as $J = sI_{inc}(\Delta F/F'_m)$ (Yin et al. 2009). Like other calibration methods, this procedure assumes that the calibration factor is the same for photorespiratory and nonphotorespiratory conditions, for which photosynthetic rates differ by a factor of $(C_c - \Gamma_*)/(C_c + 2\Gamma_*)$ (see Eqs. S1.1 and S1.3 in Supplementary Text S1; but with cautions from recent literature, Busch et al. 2018; Tcherkez and Limami 2019).

The parameter Γ_* was calculated as $0.5O_2/S_{c/o}$, where $S_{c/o}$ is the relative CO_2/O_2 specificity of Rubisco (von Caemmerer et al. 1994). Values from in vitro measurements of Cousins et al. (2010) on $S_{c/o}$ (= 3.022 mbar µbar^{-1}) and Michaelis–Menten coefficients of Rubisco for CO_2 (K_{mC} = 291 µbar) and for O_2 (K_{mO} = 194 mbar) were taken, assuming that Rubisco kinetic constants are conserved among C_3 species. This assumption was checked by in vivo estimates of $S_{c/o}$ from the lower parts of $A-C_i$ curves of five O_2 levels (see "Results").

Model method

After the above parameters were quantified, we first checked whether $g_{m,dif}$ was variable based on the combined data of gas exchange and chlorophyll fluorescence. Using measured A, C_i and a tentative value for m across its range ($0 \le m \le 1$), $g_{m,dif}$ was calculated as

$$g_{m,dif} = \frac{A + m(F + R_d)}{C_i - C_c} \quad (4)$$

where F and C_c can be solved from the A_j equation of the FvCB model, see Eq. (S1.6) in Supplementary Text S1 and Eq. (S2.1) in Supplementary Text S2, respectively. Equation (4) was derived by Yin and Struik (2017, see their Eq. 19), in analogy to the variable J method of Harley et al. (1992; also see Eq. S2.2 in Supplementary Text S2).

The obtained $g_{m,dif}$ responded to a change in both C_i and irradiance (see "Results"). Explaining these responses would need a separate study; to estimate m, here we adopted the generic phenomenological equation of Yin et al. (2009) to describe this response:

$$g_{m,dif} = g_{mo,dif} + \delta(A + R_d)/(C_c - \Gamma_*) \quad (5)$$

where $g_{mo,dif}$ and δ are parameters. If $\delta = 0$, Eq. (5) becomes a constant $g_{m,dif}$ mode ($= g_{mo,dif}$). Any nonzero δ would predict a variable $g_{m,dif}$ in response to CO_2, O_2 and irradiance levels, and if $g_{mo,dif} = 0$, parameter δ, as discussed later, represents the carboxylation: mesophyll resistance ratio. Equation (5) was combined with the FvCB and other equations to solve for A (Supplementary Text S1, where reasons for using Eq. 5 are also explained). This results in an equation expressing A as a function of C_i and other variables:

$$A = (-b \pm \sqrt{b^2 - 4ac})/(2a) \quad (6)$$

where

$$a = x_2 + \Gamma_*(1 - m) + \delta(C_i + x_2)$$

$$b = m(R_d x_2 + \Gamma_* x_1) - [x_2 + \Gamma_*(1 - m)](x_1 - R_d) - (C_i + x_2)$$
$$[g_{mo,dif}(x_2 + \Gamma_*) + \delta(x_1 - R_d)] - \delta[x_1(C_i - \Gamma_*) - R_d(C_i + x_2)]$$

$$c = -m(R_d x_2 + \Gamma_* x_1)(x_1 - R_d)$$
$$+ [g_{mo,dif}(x_2 + \Gamma_*) + \delta(x_1 - R_d)]$$
$$[x_1(C_i - \Gamma_*) - R_d(C_i + x_2)]$$

where $x_1 = V_{cmax}$ (maximum carboxylation activity of Rubisco) and $x_2 = K_{mC}(1 + O_2/K_{mO})$ for the A_c-limited conditions; $x_1 = J/4$ and $x_2 = 2\Gamma_*$ for the A_j-limited conditions, and for the A_p-limited conditions: $x_1 = 3T_p$ (where T_p is the rate of triose phosphate export from the chloroplast) and $x_2 = -(1 + 3\alpha)\,\Gamma_*$ (where α is the fraction of glycolate carbon not returned to the chloroplast).

We found that the $\sqrt{b^2 - 4ac}$ term of Eq. (6) should always take the – sign for either A_c- or A_j-limited rate, but the solution for A_p is mathematically complicated if $\alpha > 0$ (see Supplementary Text S4). Our data showed that A often declined with increasing C_i within high C_i ranges (see "Results"), suggesting the limitation by triose phosphate utilization with $\alpha > 0$ (Harley and Sharkey 1991). We conducted sensitivity analyses to choose a value of α although metabolic flux data (Abadie et al. 2018) suggest that its value might be small. We then used Eq. (6) to estimate four parameters: m ($0 \le m \le 1$), δ, V_{cmax} and T_p, by a nonlinear fitting to all data of $A - C_i$ and $A - I_{inc}$ curves of the five O_2 levels ($g_{mo,dif}$ was set to zero, see "Results"). For that, J, as defined earlier as$sI_{inc}(\Delta F/F_m')$, were used as input. Our method assumed that R_d does not vary with $[O_2]$, and was based on the expectation that neither V_{cmax} nor T_p varies with $[O_2]$, as confirmed experimentally for V_{cmax} (von Caemmerer et al. 1994). The fitting minimizes the sum of squared differences between estimated and measured A values, using the GAUSS method in PROC NLIN (SAS Institute, NC, USA). SAS scripts can be obtained upon request.

Once A was calculated from Eq. (6), C_c could be solved from Eq. (S2.1) in Supplementary Text S2. Then, $g_{m,dif}$ was re-calculated from Eq. (4) using the estimated m and measured A and C_i, where x_1 and x_2 terms were chosen according to whether the modelled A was A_c-, A_j- or A_p-limited. This showed $g_{m,dif}$ in response to CO_2, irradiance, and O_2 levels.

With $g_{m,dif}$ and other parameters, we calculated the fraction of (photo)respired CO_2 being refixed (f_{refix}), the fraction of (photo)respired CO_2 being refixed within the mesophyll cells ($f_{refix,cell}$), and the fraction of (photo)respired CO_2 being refixed via IAS ($f_{refix,ias}$), using Eqs. (S3.4), (S3.5) and (S3.6), respectively, in Supplementary Text S3. In these equations, r_{sc} is the stomatal resistance to CO_2 diffusion (being 1.6 times measured stomatal resistance to water vapour), and r_{cx} is the carboxylation resistance (which is $(C_c + x_2)/x_1$, von Caemmerer 2000). As discussed in Supplementary Text S3, these calculations need ω and λk as inputs. The estimate for m was 0.3 for tomato and 0.0 for rice (see "Results"). For tomato, we measured ω (0.65) for leaves of the same age in the same cultivar "Growdena" (see Berghuijs et al. 2015) for calculating λk, from $m = \omega\,(1 - \lambda k)$. For rice, λk was set to 1.0 to agree with the estimate that $m = 0$. In such a case, ω is not needed as Eqs. (S3.4) and (S3.5) become simplified as Eqs. (S3.3) and (S3.9) in Supplementary Text S3, respectively.

Results

Use of the five O_2 levels generated diverse shapes of photosynthetic responses to irradiance and CO_2 levels (Fig. 1). Our model approach, combined with data for A (Fig. 1) and for $\Delta F/F_m'$ (Fig. S1), yielded an estimation of a set of parameters as described below.

Estimated R_d and s

Data of $A - I_{inc}$ curves within the range of $I_{inc} \le 200$ µmol m^{-2} s^{-1} showed that the relationship between A and $(I_{inc}\Phi_2/4)$ was linear for the conditions with a gas mixture of 2% O_2 with 1000 µmol mol^{-1} C_a (Fig. 2), where Φ_2 was set to be $\Delta F/F_m'$. The value of R_d estimated from this linear relationship was 1.2 (standard error or s.e. 0.1) µmol m^{-2} s^{-1} for tomato and 1.1 (s.e. 0.1) µmol m^{-2} s^{-1} for rice. The slope of the $A - (I_{inc}\Phi_2/4)$ linearity (i.e. calibration factor s) was 0.4570 (s.e. 0.0076) for tomato and 0.5488 (s.e. 0.0076) for rice. Values of s were also re-estimated, together with other parameters, in fitting Eq. (6) to all data; but the re-estimated s remained the same, suggesting that we reached a nonphotorespiratory condition using the gas mixture.

The first few data points of the $A - C_i$ curves were linear, and gross leaf photosynthesis values $A + R_d$ were plotted versus C_i within this linear range. The intercept of this line with the C_i-axis gives the estimate of the C_i-based CO_2 compensation point, commonly noted as C_{i*}. The value of C_{i*} increased linearly with increasing O_2 levels (Fig. 3). Half of the reciprocal of this linear slope gives an in vivo estimate of $S_{c/o}$, which was 2.71 mbar µbar^{-1} for tomato and 3.13 mbar µbar^{-1} for rice. Using the method of Yin et al. (2009) gave similar in vivo estimates of $S_{c/o}$ (results not shown). These values are close to 3.02 mbar µbar^{-1} measured in vitro for wheat by Cousins

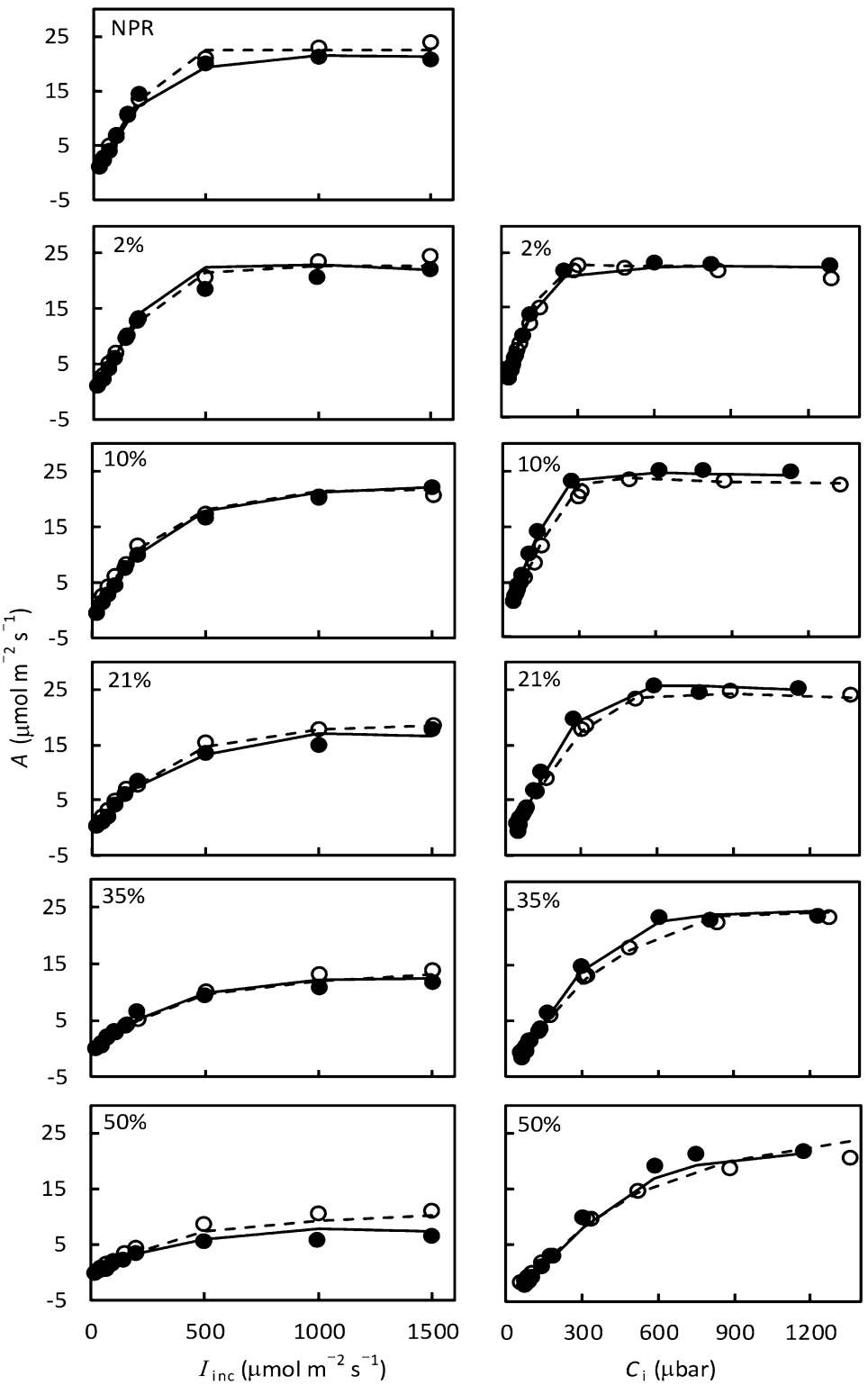

Fig. 1 Measured (points) and modelled (curves) net CO_2 assimilation rate A of tomato (filled circle, solid curves) and rice (open circle, dashed curves) as a function of incident irradiance I_{inc} (left panels) and of intercellular CO_2 concentration C_i (right panels) at different O_2 percentages as shown in individual panels. Each point represents the mean of four replicated plants. The $A - I_{inc}$ curve under nonphotorespiratory (NPR) condition was obtained at 2% O_2 combined with ambient CO_2 level of 1000 μmol mol^{-1}. Curves were drawn from connecting two nearby values calculated by the model

et al. (2010), confirming that $S_{c/o}$ is conserved among C_3 species. We will use 3.02 mbar μbar^{-1} for further analysis (but see sensitivity analysis later).

Dependence of $g_{m,dif}$ on CO_2 and irradiance level

Equation (4) assuming an electron transport limitation, was applied to check the pattern of $g_{m,dif}$ across a range of I_{inc} and C_i levels, by setting m either to 0 (equivalent to the

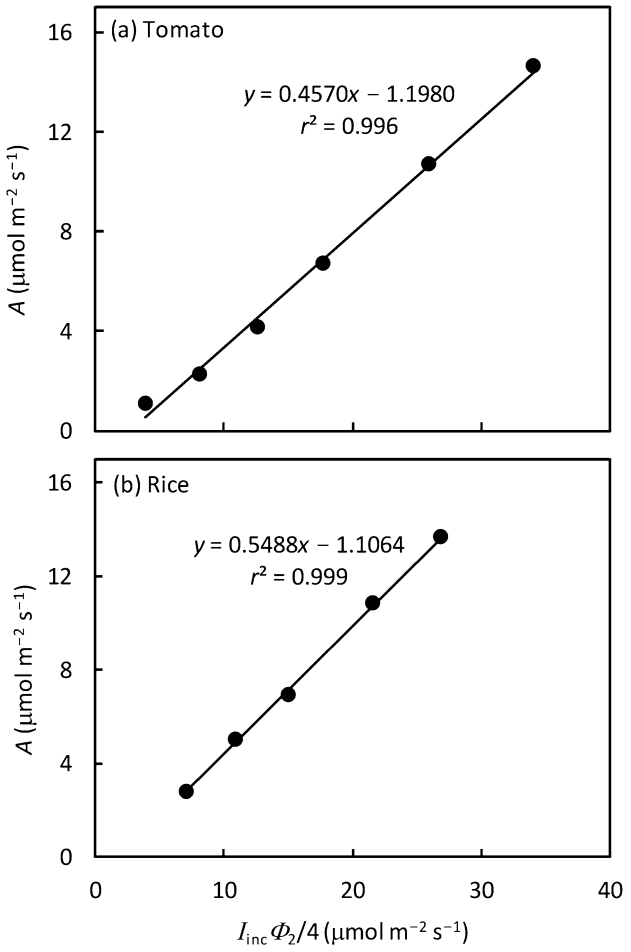

Fig. 2 Linear relationship between net CO_2 assimilation rate A and $I_{inc}\Phi_2/4$, where Φ_2 is set to be $\Delta F/F'_m$ and I_{inc} is ≤ 200 μmol m^{-2} s^{-1} (each point represents the mean of measurements on leaves from four replicated plants), for nonphotorespiratory condition (2% O_2 combined with $C_a = 1000$ μmol mol^{-1}). The intercept of regression lines gives an estimate of $-R_d$ (see Yin et al., 2011), and the slope gives an estimate of the calibration factor s for converting $\Delta F/F'_m$ into the linear electron transport rates (see the text)

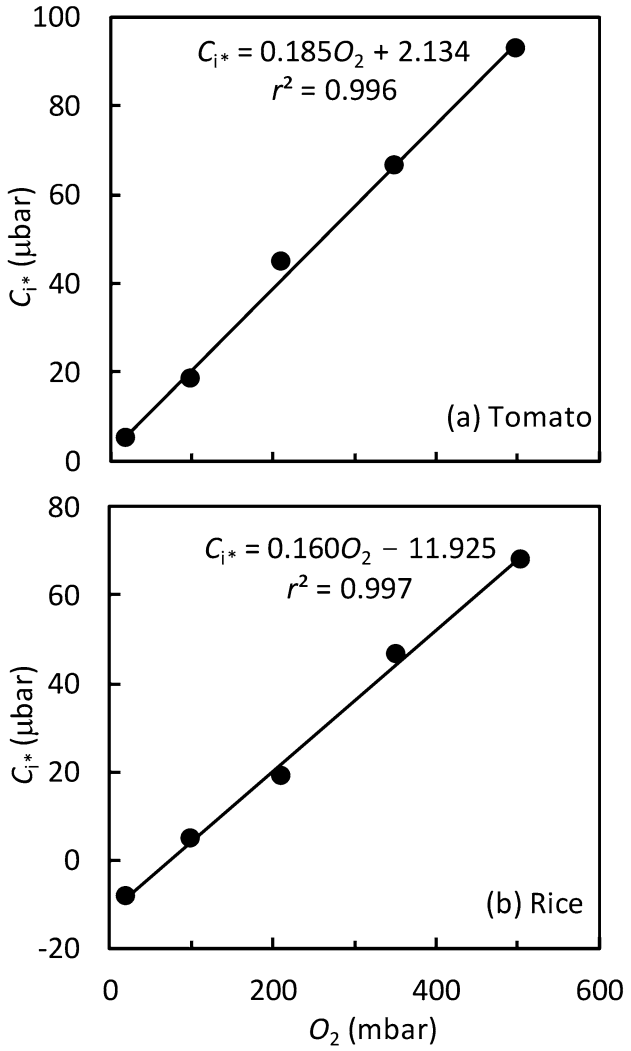

Fig. 3 Values of CO_2 compensation point C_{i*} [identified as the intercept at the C_i-axis of the initial strictly linear part of leaf gross CO_2 assimilation rate $(A + R_d)$ versus C_i] plotted as a function of the O_2 levels, for tomato and rice leaves

variable J method of Harley et al. (1992) for $g_{m,app}$) or to a value between 0 and 1. A similar response was obtained for various O_2 levels, except for 2% O_2. At that oxygen concentration, Eq. (4), like the variable J method, cannot be reliably applied due to insufficient photorespiration (see Supplementary Text S2). Although the obtained $g_{m,dif}$ sometimes had unrealistic values largely due to unrealistic values of C_c (as often occurs when using the variable J method, see Yin and Struik 2009), an overall trend of $g_{m,dif}$ in response to I_{inc} and to C_i was obtained. An example of the response is shown in Fig. 4 for the case of 10% O_2 level for tomato. $g_{m,dif}$ increased monotonically with increasing I_{inc} (Fig. 4a), and decreased gradually with an increase in C_i (Fig. 4b). Changing m did not change the response pattern, but only the absolute value of $g_{m,dif}$, and a nonzero m resulted in higher $g_{m,dif}$ than the value obtained from setting $m = 0$ (Fig. 4).

Estimates of parameters δ, m, V_{cmax} and T_p

Equation (6) for describing A was applied to estimate $g_{mo,dif}$, δ and m, using data of both $A - I_{inc}$ and $A - C_i$ curves. The obtained $g_{mo,dif}$ did not differ significantly from zero ($p > 0.05$), which is supported by the result that the calculated $g_{m,dif}$ by Eq. (4) at low I_{inc} was close to zero (Fig. 4a). Also, model fit became worse if δ was fixed to zero than if $g_{mo,dif}$ was fixed to zero, supporting the variable $g_{m,dif}$ mode. Sensitivity analysis with respect to α suggested that a change within its relevant range had no impact on the estimates of parameters other than T_p (see below). We set $g_{mo,dif}$ to

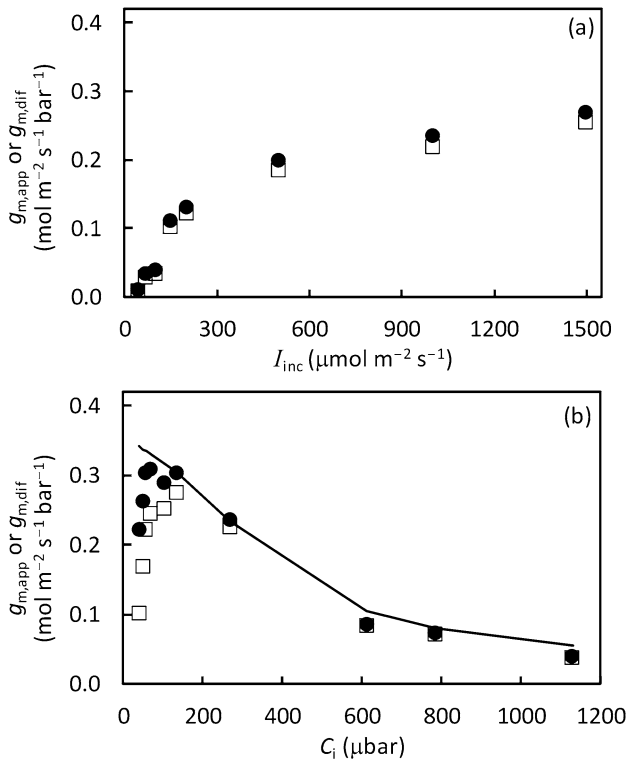

Fig. 4 Calculated $g_{m,app}$ using the variable J method of Harley et al. (1992) (open square) or $g_{m,dif}$ using Eq. (4) where parameter m is set to 0.29 (filled circle), as a function of **a** incident irradiance I_{inc} or **b** intercellular CO_2 level C_i, under the condition of 10% O_2 for tomato leaves. Points were obtained, based on the A_j part of the FvCB model, using measured A and J that was derived from chlorophyll fluorescence with the calibration as described in the text. The monotonically descending curve in panel (b) is drawn from values of the modelled $g_{m,dif}$ using the full FvCB model of three limited rates

zero, and α to 0.3 (Busch and Sage 2017), in the subsequent analysis.

Equation (6) describes well both $A-I_{inc}$ and $A-C_i$ curves (Fig. 1), with an overall R^2 being > 0.99 for either species (Table 2). Most of the data points (> 80%) were A_j-limited, indicating that chlorophyll fluorescence signals generally echoed gas exchange data since we calculated J from chlorophyll fluorescence measurements as $sI_{inc}(\Delta F/F'_m)$. Only a few points at low C_i of $A-C_i$ curves or at high I_{inc} of $A-I_{inc}$ curves were A_c-limited, and a few points at high C_i of $A-C_i$ curves under low O_2 conditions were A_p-limited. The estimated m was ca 0.3 for tomato but was 0.0 for rice (Table 2). The estimated δ was also higher for tomato (1.4) than for rice (1.0) (Table 2). Other parameter values were similar for the two species: 113.7 and 111.0 μmol m^{-2} s^{-1} for V_{cmax}, and 8.3 and 7.8 μmol m^{-2} s^{-1} for T_p, for tomato and rice, respectively.

Sensitivity analysis

Given that any uncertainty in estimated s and R_d and in other parameters ($S_{c/o}$, K_{mC}, K_{mO} and α) may have an impact on the major estimated parameters (m and δ in this study), we carried out sensitivity analyses. The estimation of δ and m was very sensitive to s and $S_{c/o}$, and less sensitive to R_d (Fig. S2), but virtually insensitive to K_{mC}, K_{mO} and α (results not shown). Both δ and m decreased monotonically with increasing s (Fig. S2a). The estimate of δ decreased with increasing $S_{c/o}$, whereas that of m changed in an opposite direction (Fig. S2b). The obtained response of δ (the parameter in Eq. (5) on mesophyll conductance) to both $S_{c/o}$ and s is expected in the same way as $g_{m,app}$ responds to these parameters (Harley et al. 1992). The opposite response of m to $S_{c/o}$ and s is probably because photorespiration, i.e. the F term in Eq. (3), which is relevant to determining m, has an opposite response to $S_{c/o}$ and s. As R_d has the same effect as the F term has (see Eq. 3), the estimated m decreased with increasing R_d, whereas δ changed in an opposite direction (Fig. S2c). As expected, any sensitivity to K_{mC} and K_{mO} occurred with the estimated V_{cmax}, whereas a sensitivity to α occurred with T_p (results not shown).

Table 2 Estimates (standard errors in brackets) of two major parameters (δ and m), and V_{cmax} and T_p, from fitting Eq. (6) to irradiance- and CO_2 response curves of five O_2 levels for leaves of tomato and rice

Parameter	Unit	Estimates	
		Tomato	Rice
δ (a coefficient defining variations in $g_{m,dif}$)	–	1.41 (0.09)	1.03 (0.05)
m (lumped anatomical-feature parameter)	–	0.29 (0.07)	0.00
V_{cmax} (maximum rate of Rubisco activity) [a]	μmol m^{-2} s^{-1}	113.70 (3.51)	111.0 (6.44)
T_p (rate of triose phosphate utilization) [b]	μmol m^{-2} s^{-1}	8.31 (0.11)	7.81 (0.06)
R^2	–	0.992	0.993

[a]Sensitivity analysis showed that only the estimate of V_{cmax} depends on values of K_{mC} and K_{mO} (see text); here V_{cmax} was estimated using K_{mC} = 291 μbar and K_{mO} = 194 mbar (Cousins et al. 2010)

[b]Sensitivity analysis showed that only the estimate of T_p depends on the value of α (see text); here T_p was estimated assuming that α = 0.3 (Busch and Sage 2017)

Calculated fractions for re-assimilation of (photo) respired CO_2

The calculated fractions of (photo)respired CO_2 being refixed, using Eqs. (S3.4–S3.6) in Supplementary Text S3, are shown in Fig. 5, using the result at 21% O_2 as the example. The trends were similar for O_2 levels above 2%. Except for very low I_{inc} or C_i levels, the refixed fractions were quite consistent over a wide range of conditions. $f_{refix,cell}$ was lower in tomato (0.25) than in rice (0.49) (Fig. 5), largely due to the fact that the estimated m was 0.3 for tomato but 0.0 for rice (Table 2). In contrast, $f_{refix,ias}$ was higher in tomato than in rice. As a result, the total re-fixation fraction f_{refix} was comparable for the two species, i.e. up to ca 0.6.

Responses of stomatal and mesophyll conductance to O_2

Except for a few cases, g_{sc} generally decreased with increasing [O_2], and was lower in tomato than in rice (Fig. 6). The calculated value of $g_{m,dif}$ also decreased with increasing [O_2], except for very high CO_2 conditions which lowered $g_{m,dif}$ to the extent that the O_2 response of $g_{m,dif}$ was no longer significant (Fig. 6d,j). $g_{m,dif}$ was higher in tomato than in rice.

Discussion

Analysing mesophyll resistance

Compared with the CO_2 flux coming from IAS, (photo) respired CO_2 experiences different resistances. This suggests the need to dissect $r_{m,dif}$ into sub-components. Anatomical measurements can partition mesophyll resistance into individual sub-components (Peguero-Pina et al. 2012; Tosens et al. 2012a, b; Tomas et al. 2013; Carriquí et al. 2019). The calculation of these sub-components relies on many assumed diffusion or permeability coefficients that are uncertain (Berghuijs et al. 2015). Furthermore, this approach does not quantify the effect of the arrangement of mitochondria and chloroplasts on the intracellular CO_2 diffusion.

In line with anatomical measurements, Eq. (2) dissects $r_{m,dif}$ into two sub-components r_{wp} and r_{ch} (Tholen et al. 2012). Oxygen isotope techniques may estimate r_{wp} based on certain assumptions (Barbour 2017), but so far have been explored to separate r_{wp} and r_{ch} within the framework of the classical g_m model, Eq. (1) (Barbour et al. 2016b). Equations (1) and (2) both underrepresent the intracellular arrangements of organelles. In contrast, the model of Yin and Struik (2017), Eq. (3), has a factor lumping (i) the

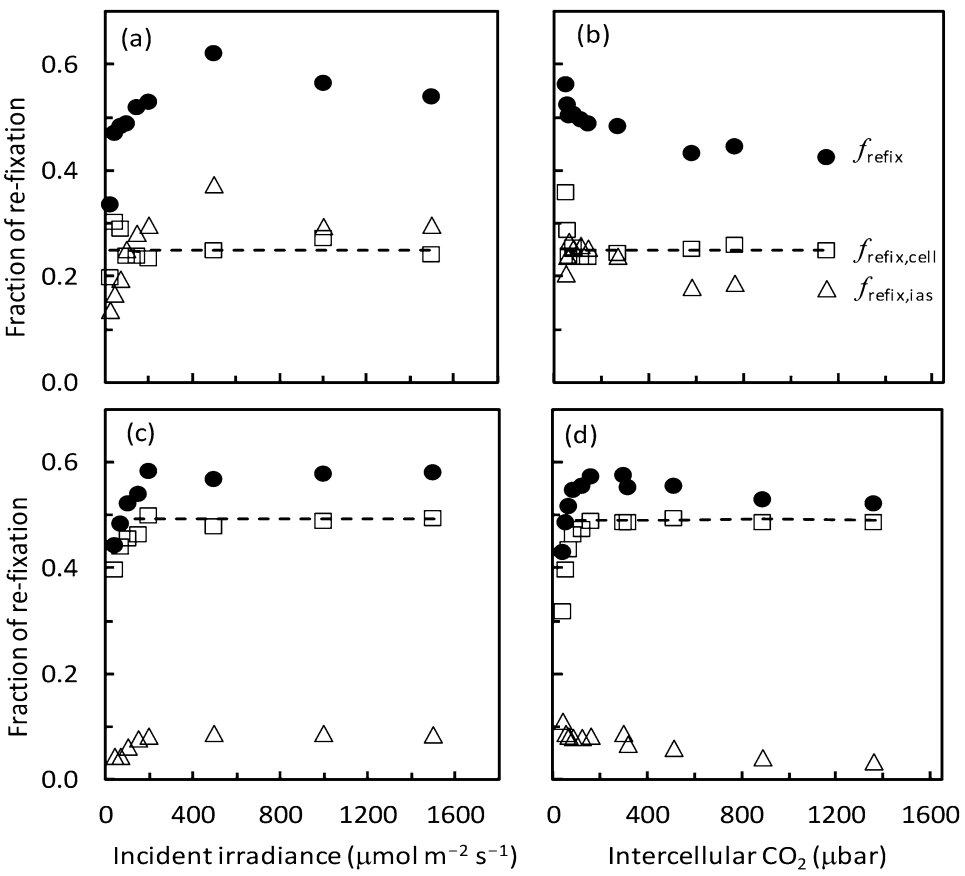

Fig. 5 Calculated fractions of total re-assimilation (filled circle, f_{refix}), of re-assimilation within mesophyll cells (open square, $f_{refix,cell}$), and of re-assimilation via the intercellular air spaces (open triangle, $f_{refix,ias}$) at different incident irradiance (**a**, **c**) or intercellular CO_2 (**b**, **d**) levels, in leaves of tomato (**a**, **b**) and rice (**c**, **d**), when the O_2 level was 21%. The horizontal dashed line represents the calculated $f_{refix,cell}$ using the model predicted A values. In the calculation for tomato, we used the value of ω (the proportion of r_{ch} in total $r_{m,dif}$) of 0.65 that we measured, as reported by Berghuijs et al. (2015, see the text)

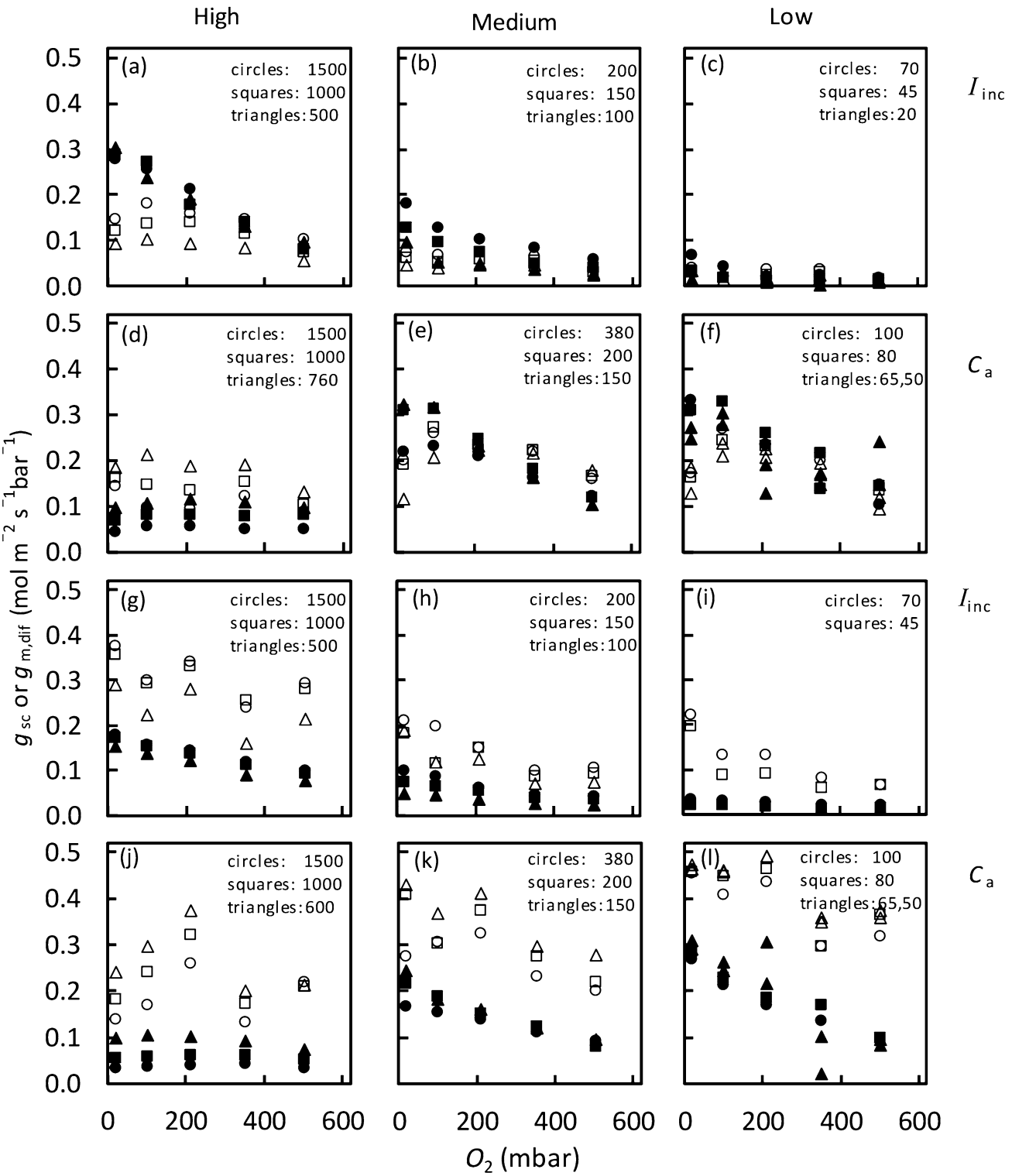

Fig. 6 Stomatal conductance for CO_2 diffusion g_{sc} (open symbols) and mesophyll conductance $g_{m,dif}$ (closed symbols) of tomato (**a–f**) and rice (**g–l**) leaves in response to O_2 level, at high (left panels), medium (middle panels) and low (right panels) I_{inc} levels (**a–c**, **g–i**) or C_a levels (**d–f**, **j–l**). Values of I_{inc} or C_a are shown at each corresponding panels, where units of I_{inc} and C_a are μmol m^{-2} s^{-1} and μmol mol^{-1}, respectively

r_{ch}:$r_{m,dif}$ ratio (ω), (ii) the fraction of (photo)respired CO_2 that are released in the inner cytosol (λ), and (iii) k, the factor for the change in λ as a result of the chloroplast gaps. The factor k is particularly hard to assess. Since ω, λ and k lump as such that $m = \omega\ (1 - \lambda k)$, Eq. (3) provides an approach by exploring nondestructive gas exchange and chlorophyll fluorescence measurements under different levels of O_2 that created large variations in photorespiration. Instead of estimating individual resistances, our nonlinear fitting approach estimates $r_{m,dif}$ as a whole, as well as the m factor. Common nonlinear procedures, typically by fitting $A - C_i$ curves, estimate four or even more parameters of the FvCB model, such as V_{cmax}, J, T_p, and g_m (e.g. Sharkey et al. 2007). In our method, J was measured from chlorophyll fluorescence. Despite a wide range of O_2 levels exploited, we restricted the number of estimated parameters to four from Eq. (6)-based nonlinear fitting. All four were reliably estimated for both species with small standard errors (Table 2).

Our approach is still a simplified representation of complex diffusion pathways. Some respiratory flux may originate in the chloroplasts, in cytosol, and in the heterotrophic tissues such as epidermis, vasculature, and bundle sheath (Tcherkez et al. 2017). These components of R_d could be incorporated as additional terms into the C_i–C_c gradient equation, Eq. (S1.7) in Supplementary Text S1. However, they are ignored here as fractions of these components in R_d are generally unknown. There may also be some activity of phospho*enol*pyruvate carboxylase (V_{pepc}) in cytosol (Douthe et al. 2012; Abadie and Tcherkez 2019), which would counteract the effect of $(F + R_d)$ on $g_{m,app}$. But our procedure of estimating R_d may have accounted for this, i.e. the estimated R_d represents the net rate of true R_d minus V_{pepc}. Tholen et al. (2012) showed that small amounts of V_{pepc} have little impact on $g_{m,app}$.

Variation of $g_{m,dif}$ with CO_2, irradiance and O_2 levels

Reports using chlorophyll fluorescence data consistently showed that $g_{m,app}$ initially increases and then decreases with increasing C_i and increases monotonically with increasing I_{inc} (e.g. Flexas et al. 2007a; Yin et al. 2009). Similar results for $g_{m,app}$ in response to C_i (Vrábl et al. 2009; Tazoe et al. 2011) and to I_{inc} (Douthe et al. 2012) were sometimes reported, using the carbon isotope discrimination method. No change in anatomical arrangements was observed that could explain the variable $g_{m,app}$ (Carriquí et al. 2019). Gu and Sun (2014) showed that the reported response of $g_{m,app}$ to a change in CO_2 or in I_{inc} may be due to the artefact of errors in experimental measurements. Although resolving experimental uncertainties is urgently needed, consistent variations of $g_{m,app}$ cannot be ascribed only to experimental errors because responses due to random errors would be irregular and inconsistent among various reports. Théroux-Rancourt and Gilbert (2017) demonstrated that changing patterns of light penetration within the leaf 3D-structure leads to different contributions of each cell layer to bulk-leaf mesophyll conductance, resulting in an apparent response of the bulk-leaf $g_{m,app}$ to light intensity. However, their theory cannot explain the response of $g_{m,app}$ to C_i.

Most results using the variable J method of Harley et al. (1992) showed that within a low C_i range, $g_{m,app}$ typically decreases with decreasing C_i (e.g. Flexas et al. 2007a; Vrábl et al. 2009; Yin et al. 2009; Fig. 4b). Tholen et al. (2012) also noted a decrease of $g_{m,app}$ with increasing O_2 level. Tholen et al. (2012) explained these responses to C_i and O_2 as a consequence of the fact that $g_{m,app}$ as an apparent parameter decreases with an increase in the $(F + R_d)/A$ ratio. If this is the only explanation of variable $g_{m,app}$, one would expect that $g_{m,dif}$ would be independent of C_i because Eq. (4) for $g_{m,dif}$ already accounts for the $(F + R_d)/A$ ratio. However, $g_{m,dif}$ still declined with decreasing C_i within its low range, albeit to a lesser extent (Fig. 4b). In fact, within the low C_i range, A is limited by Rubisco activity; so, as noted by Yin et al. (2009), using the variable J method or Eq. (4) assuming an electron transport limitation results in an artefactual decline of estimated g_m because the occurrence of additional alternative electron transport is wrongly attributed to the mesophyll diffusional limitation. This assertion was supported by the result that the decrease of $g_{m,dif}$ with decreasing C_i within the low C_i range was no longer obtained once $g_{m,dif}$ was calculated from the full FvCB model (Fig. 4b). This suggests that the decrease of $g_{m,app}$ with decreasing C_i is explained more by the occurrence of alternative electron transport than by the theory of Tholen et al. Anyway, the theory does not explain the decreases of $g_{m,app}$ with increasing C_i within its high range, or with decreasing I_{inc}, or with lowering temperature as reported previously (Bernacchi et al. 2002; Warren and Dreyer 2006; Yamori et al. 2006; Scafaro et al. 2011; Evans and von Caemmerer 2013).

We found that $g_{m,dif}$ increased with I_{inc} (Fig. 4a). This increase continued within the high I_{inc} range, where some additional alternative electron transport is also expected, suggesting that the increase of $g_{m,dif}$ with I_{inc} overrode any artefactual decline caused by alternative electron fluxes. Also, $g_{m,dif}$ decreased with increasing O_2 (Fig. 6), in the same direction as the O_2 response of $g_{m,app}$ reported by Tholen et al. (2012). Literature on O_2 responses of diffusional conductance is scarce (Farquhar and Wong 1984; Buckley et al. 2003). Our data showed that both g_{sc} and $g_{m,dif}$ generally declined with increasing O_2. So, $g_{m,dif}$ is variable, in response to C_i, I_{inc}, and O_2, in a similar pattern as g_{sc} responds to these variables (e.g. Morison and Gifford 1983; Farquhar and Wong 1984; Buckley et al. 2003).

The identified variable $g_{m,dif}$ was based on the assumption that m ($= \omega$ (1-λk)) is constant, independent of short-term changes (within 3–8 min) in irradiance or [CO_2]. This is

supported by Carriquí et al. (2019), who reported that anatomical parameters determining ω and k hardly vary with short-term changes in irradiance or [CO_2]. Chloroplasts and mitochondria in some plants may move under varying light, but they always colocalize (Islam et al. 2009), suggesting that λ also hardly varies. We are unable to find evidences supporting quantitative changes that m or its components must have to obtain invariable $g_{m,dif}$ with irradiance, [CO_2] and [O_2].

$g_{m,dif}$ defined here is still a bulk-leaf trait. Like bulk-leaf $g_{m,app}$, it may not represent intrinsic transport properties. Also, our result on the variable $g_{m,dif}$ is subject to experimental confirmation by other methods. If proven true, future studies are needed to examine if the variable $g_{m,dif}$ can emerge from fluxes and concentrations across the real 3D-structure of leaves, as well as in relation to membrane permeability and other properties. Here we only describe the response from bulk-leaf equations themselves. $g_{m,dif}$ can be formulated from Eq. (4) and $A = V - F - R_d$ (where V is the carboxylation rate) as

$$g_{m,dif} = \frac{V - (1-m)(F + R_d)}{C_i(1 - C_c : C_i)} \quad (7)$$

When I_{inc} increases, only the numerator increases significantly; so Eq. (7) predicts that $g_{m,dif}$ increases with increasing I_{inc}. If the CO_2 gradient from C_i and C_c is regulated such that the C_c:C_i ratio is roughly constant for a given O_2 level (results not shown), Eq. (7) also predicts that $g_{m,dif}$ will decrease monotonically with C_i because according to the FvCB model, the V increment per C_i increment decreases with increasing C_i. Finally, the F term increases when O_2 increases; as a result, Eq. (7) predicts that $g_{m,dif}$ decreased with increasing O_2 (Fig. 6).

Interpretation of the model and estimated parameter values

Our method is based on Eq. (3), the equation summarized by Yin and Struik (2017) from considering six possible scenarios for the intracellular organelle arrangement. Recently, Ubierna et al. (2019) came up with the same model but formulated $g_{m,app}$ in a Michaelis–Menten-like equation, i.e. $g_{m,app} = A \cdot g_{m,dif} / [A + m(F + R_d)]$ (see their Eq. 15; note that $g_{m,app}$ was written as g_m in their notations). The maximum value of $g_{m,app}$ is $g_{m,dif}$, while the Michaelis–Menten constant "K_m" is $m(F + R_d)$. For the case of tomato where $m = 0.3$ and $R_d = 1.2$, the "K_m" occurs at $A \approx 2.0$ µmol m^{-2} s^{-1} for the ambient O_2 condition. This suggests that $g_{m,app}$ and $g_{m,dif}$ only differ significantly when A is low, which our results (Fig. 4) confirmed.

In view of the variation of $g_{m,dif}$ shown in Fig. 4, we adopted Eq. (5), which accommodates either constant or variable $g_{m,dif}$ in relation to C_i, I_{inc} and O_2 levels. Although the equation is phenomenological and has an a priori assumption that $g_{m,dif}$ grows with relative carboxylation and the estimates of its parameters are expectedly sensitive to the pre-input values of s, $S_{c/o}$ and R_d (Fig. S2), the model generated useful insights.

Our results supported no constant $g_{m,dif}$, but a variable $g_{m,dif}$ with parameter δ being 1.0 for rice and 1.4 for tomato (Table 2). Equation (5) with $g_{mo,dif} = 0$ for our variable $g_{m,dif}$ mode can be rewritten to $r_{m,dif} = (C_c - \Gamma_*)/[\delta(A + R_d)]$. As $(A + R_d)$ can be calculated from the FvCB model as $(C_c - \Gamma_*)x_1/(C_c + x_2)$, the above equation becomes $r_{m,dif} = (C_c + x_2)/(\delta x_1)$. As $(C_c + x_2)/x_1$ is defined as carboxylation resistance r_{cx} (von Caemmerer 2000), it follows that

$$\delta = r_{cx}/r_{m,dif.} \quad (8)$$

Thus, parameter δ of Eq. (5) has a meaning, representing the carboxylation: mesophyll resistance ratio. Our estimates for δ (Table 2) suggest that r_{cx} and $r_{m,dif}$ had similar values in rice leaves, whereas r_{cx} was ca 40% higher than $r_{m,dif}$ in tomato leaves.

Our estimate of the factor m was ca 0.3 for tomato and 0.0 for rice (Table 2). Thus, using Eq. (1), which is the special case of the generalized model when $m = 0$, actually suits for rice leaves but does not work for tomato leaves when $(F + R_d)/A$ is high. As stated in Introduction, the classical model works well if mitochondria are located exclusively in the inner cytosol ($\lambda = 1$) and chloroplasts cover fully the mesophyll periphery that $k = 1$. Sage and Sage (2009) and Busch et al. (2013) showed that compared with other species, in rice leaves, there are stromules that effectively extend chloroplast coverage of the cell periphery and mitochondria locate in the cell interior and are intimately associated with chloroplasts/stromules. These features engender such a structure as if (photo)respired CO_2 is released in the same compartment where RuBP carboxylation occurs. This is the case when Eq. (1) works well. Therefore, our results with curve-fitting to gas exchange data actually agree with anatomical differences between species.

Such differences are also shown in the fractions of re-fixation of (photo)respired CO_2 calculated from resistance components (Fig. 5). With the distinct anatomical feature of rice leaves, (photo)respired CO_2, if to exit mesophyll cells, will have to travel via the stroma, thereby maximizing the re-fixation of (photo)respired CO_2 within the cell. Therefore, rice had higher values of $f_{refix,cell}$ than tomato (Fig. 5). For a given set of resistance values, the organelle arrangements as in rice leaves that make the highest $f_{refix,cell}$ can result in low $f_{refix,ias}$ (see Supplementary Text S3). Moreover, in line with the observation of Ouyang et al. (2017) on rice 'IR64', the cultivar we used, rice had high stomatal

conductance, compared with tomato (Fig. 6). A low g_{sc} would make (photo)respired CO_2 more difficult to exit into the atmosphere via IAS. This also contributed to higher values of $f_{refix,ias}$ in tomato than in rice (Fig. 5). As a result, the two species had similar values (up to 60%) of the total refixation, f_{refix}. The calculated $f_{refix,ias}$ and f_{refix} varied with I_{inc} or C_i levels (Fig. 5), because resistance components r_{sc} and r_{cx} varied with these variables. The calculated $f_{refix,cell}$ was more constant (Fig. 5). Substituting Eq. (8) into Eq. (S3.5) in Supplementary Text S3 gives

$$f_{refix,cell} = \frac{(1-\omega)(\delta+\omega\lambda k)}{(1+\delta)[\delta-\omega\lambda k(\delta+\omega-1)]} \quad (9)$$

As all terms are constant, Eq. (9) describes why $f_{refix,cell}$ stayed invariant. Using isotope mass spectrometry and gas exchange measurements, Busch et al. (2013) determined $f_{refix,cell}$, $f_{refix,ias}$ and f_{refix}, being 0.29, 0.22, and 0.51 for rice under ambient CO_2 and high light conditions. Our estimates for rice somewhat differed from their values for comparable conditions (Fig. 5d).

The difference in the value of factor m between the species also has implications on values of C_{i*} and the relationship between C_{i*} and Γ_*. C_{i*} was lower in rice than in tomato at a given O_2 level (Fig. 3), and C_{i*} at the lowest O_2 in rice was even negative (Fig. 3b). A negative C_{i*} could be due to measurement noises, uncertainties in assuming constant R_d, and the influence of varying amounts of V_{pepc} (see earlier discussions). However, for the case where $m=0$, it can be seen from Eq. (1) that $C_{i*}=\Gamma_* - R_d/g_m$ (von Caemmerer et al. 1994); so, C_{i*} is always lower than Γ_*. This agrees with our linear relation for rice in Fig. 3b (where the term $0.16O_2$ can be considered as Γ_*, given that $\Gamma_*=0.5O_2/S_{c/o}$). Setting the intercept of this relation equal to $-R_d/g_m$ and knowing that $R_d=1.064$ μmol m^{-2} s^{-1} (Fig. 2b), g_m for rice can be solved as ca 0.1 mol m^{-2} s^{-1} bar^{-1}, comparable with its value calculated in the other way for low CO_2 conditions (Fig. 6l). So, a negative C_{i*} for low O_2 conditions could actually represent biological realities, i.e. high intracellular refixation of both respired CO_2 and photorespired CO_2 sufficed to (over)compensate for photorespiratory losses. In contrast, for cases where $m \geq 0$, the relation between C_{i*} and Γ_* can be formulated from Eq. (S1.7) in Supplementary Text S1 as

$$C_{i*} = \Gamma_* - [(1-m)R_d - mF]/g_{m,dif} \quad (10)$$

Equation (10) means that C_{i*} is no longer necessarily lower than Γ_* (see also Tholen et al. 2012), depending on relative values of $(1–m)R_d$ versus mF. Our result in Fig. 3a suggests that C_{i*} is 2.134 μbar higher than Γ_* for tomato. Thus, different m values estimated by curve-fitting for the two species are supported by the C_{i*} vs Γ_* relationships in Fig. 3, suggesting that our approach is internally consistent.

Compliance with Ethical Standards

Conflict of interest The authors declare that they have no conflict of interest.

References

Abadie C, Tcherkez G (2019) In vivo phospho*enol*pyruvate carboxylase activity is controlled by CO_2 and O_2 mole fractions and represents a major flux at high photorespiration rates. New Phytol 221:1843–1852

Abadie C, Bathellier C, Tcherkez G (2018) Carbon allocation to major metabolites in illuminated leaves is not just proportional to photosynthesis when gaseous conditions (CO_2 and O_2) vary. New Phytol 218:94–106

Barbour MM (2017) Understanding regulation of leaf internal carbon and water transport using online stable isotope techniques. New Phytol 213:85–88

Barbour M, Bachmann S, Bansal U, Bariana H, Sharp P (2016a) Genetic control of mesophyll conductance in common wheat. New Phytol 209:461–465

Barbour MM, Evans JR, Simonin KA, von Caemmerer S (2016b) Online CO_2 and H_2O oxygen isotope fractionation allows estimation of mesophyll conductance in C_4 plants, and reveals that mesophyll conductance decreases as leaves age in both C_4 and C_3 plants. New Phytol 210:875–889

Berghuijs HNC, Yin X, Ho QT, van der Putten PEL, Verboven P, Retta MA, Nicolaï BM, Struik PC (2015) Modelling the relationship between CO_2 assimilation and leaf anatomical properties in tomato leaves. Plant Sci 238:297–311

Bernacchi CJ, Portis AR, Nakano H, von Caemmerer S, Long SP (2002) Temperature response of mesophyll conductance. Implication for the determination of Rubisco enzyme kinetics and for limitations to photosynthesis in vivo. Plant Physiol 130:1992–1998

Buckley TN, Mott KA, Farquhar GD (2003) A hydromechanical and biochemical model of stomatal conductance. Plant Cell Environ 26:1767–1785

Busch FA, Sage RF (2017) The sensitivity of photosynthesis to O_2 and CO_2 concentration identifies strong Rubisco control above the thermal optimum. New Phytol 213:1036–1051

Busch FA, Sage TL, Cousins AB, Sage RF (2013) C_3 plants enhance rates of photosynthesis by reassimilating photorespired and respired CO_2. Plant Cell Environ 36:200–212

Busch FA, Sage RF, Farquhar GD (2018) Plants increases CO_2 uptake by assimilating nitrogen via the photorespiratory pathway. Nat Plants 4:46–54

Carriquí M, Douthe C, Molins A, Flexas J (2019) Leaf anatomy does not explain apparent short-term responses of mesophyll conductance to light and CO_2 in tobacco. Physiol Plant 165:604–618

Cousins AB, Ghannoum O, von Caemmerer S, Badger MR (2010) Simultaneous determination of Rubisco carboxylase and oxygenase kinetic parameters in *Triticum aestivum* and *Zea mays* using membrane inlet mass spectrometry. Plant Cell Environ 33:444–452

Douthe C, Dreyer E, Brendel O, Warren CR (2012) Is mesophyll conductance to CO_2 in leaves of three *Eucalyptus* species sensitive to short-term changes of irradiance under ambient as well as low O_2? Funct Plant Biol 39:435–448

Evans JR, von Caemmerer S (2013) Temperature response of carbon isotope discrimination and mesophyll conductance in tobacco. Plant Cell Environ 36:745–756

Evans JR, von Caemmerer S, Setchell BA, Hudson GS (1994) The relationship between CO_2 transfer conductance and leaf anatomy in transgenic tobacco with a reduced content of Rubisco. Aust J Plant Physiol 21:475–495

Evans JR, Kaldenhoff R, Genty B, Terashima I (2009) Resistances along the CO_2 diffusion pathway inside leaves. J Exp Bot 60:2235–2248

Farquhar GD, Wong SC (1984) An empirical model of stomatal conductance. Aust J Plant Physiol 11:191–210

Farquhar GD, von Caemmerer S, Berry JA (1980) A biochemical model of photosynthetic CO_2 assimilation in leaves of C_3 species. Planta 149:78–90

Flexas J, Diaz-Espejo A, Galmes J, Kaldenhoff R, Medrano H, Ribas-Carbó M (2007a) Rapid variation of mesophyll conductance in response to changes in CO_2 concentration around leaves. Plant Cell Environ 30:1284–1298

Flexas J, Diaz-Espejo A, Berry JA, Cifre J, Galmes J, Kaldenhoff R, Medrano H, Ribas-Carbó M (2007b) Analysis of leakage in IRGA's leaf chambers of open gas exchange systems: quantification and its effects in photosynthesis parameterization. J Exp Bot 58:1533–1543

Genty B, Briantais J-M, Baker N (1989) The relationship between the quantum yield of photosynthetic electron transport and quenching of chlorophyll fluorescence. Biochem Biophys Acta 990:87–92

Gu L, Sun Y (2014) Artefactual responses of mesophyll conductance to CO_2 and irradiance estimated with the variable J and online isotope discrimination methods. Plant Cell Environ 37:1231–1249

Harley PC, Sharkey TD (1991) An improved model of C_3 photosynthesis at high CO_2: Reversed O_2 sensitivity explained by lack of glycerate reentry into the chloroplast. Photosynth Res 27:169–178

Harley PC, Loreto F, Di Marco G, Sharkey TD (1992) Theoretical considerations when estimating the mesophyll conductance to CO_2 flux by analysis of the response of photosynthesis to CO_2. Plant Physiol 98:1429–1436

Hatakeyama Y, Ueno O (2016) Intracellular position of mitochondria and chloroplasts in bundle sheath and mesophyll cells of C_3 grasses in relation to photorespiratory CO_2 loss. Plant Prod Sci 19:540–551

Islam MS, Niwa Y, Takagi S (2009) Light-dependent intracellular positioning of mitochondria in *Arabidopsis thaliana* mesophyll cells. Plant Cell Physiol 50:1032–1040

Kebeish R, Niessen M, Thirshnaveni K, Bari R, Hirsch H-J, Rosenkranz R, Stäbler N, Schönfeld B, Kreuzaler F, Peterhänsel C (2007) Chloroplastic photorespiratory bypass increases photosynthesis and biomass production in *Arabidopsis thaliana*. Nat Biotechnol 25:593–599

Laisk A, Eichelmann H, Oja V, Rasulov B, Rämma H (2006) Photosystem II cycle and alternative electron flow in leaves. Plant Cell Physiol 47:972–983

Loriaux SD, Avenson TJ, Wells JM, McDermitt DK, Eckles RD, Riensche B, Genty B (2013) Closing in on maximum yield of chlorophyll fluorescence using a single multiphase flash of subsaturating intensity. Plant Cell Environ 36:1755–1770

Morison JIL, Gifford RM (1983) Stomatal sensitivity to carbon dioxide and humidity. Plant Physiol 71:789–796

Ouyang W, Struik PC, Yin X, Yang J (2017) Stomatal conductance, mesophyll conductance, and transpiration efficiency in relation to leaf anatomy in rice and wheat genotypes under drought. J Exp Bot 68:5191–5205

Peguero-Pina JJ, Flexas J, Galmes J, Niinemets Ü, Sancho-Knapik D, Barredo G, Villarroya D, Gil-Pelegrin E (2012) Leaf anatomical properties in relation to differences in mesophyll conductance to CO_2 and photosynthesis in two related Mediterranean *Abies* species. Plant Cell Environ 35:2121–2129

Sage TL, Sage RF (2009) The functional anatomy of rice leaves: Implications for refixation of photorespiratory CO_2 and effects to engineer C_4 photosynthesis into rice. Plant Cell Physiol 50:756–772

Scafaro AP, von Caemmerer S, Evans JR, Atwell BJ (2011) Temperature response of mesophyll conductance in cultivated and wild *Oryza* species with contrasting mesophyll cell wall thickness. Plant Cell Environ 34:1999–2008

Sharkey TD (1985) O_2-insensitive photosynthesis in C_3 plants: Its occurrence and a possible explanation. Plant Physiol 78:71–75

Sharkey TD, Bernacchi CJ, Farquhar GD, Singsaas EL (2007) Fitting photosynthetic carbon dioxide response curves for C_3 leaves. Plant Cell Environ 30:1035–1040

Sun Y, Gu L, Dickinson RE, Norby RJ, Pallardy SG, Hoffman FM (2014) Impact of mesophyll diffusion on estimated global land CO_2 fertilization. Proc Natl Acad Sci USA 111:15774–15779

Tazoe Y, von Caemmerer S, Badger MR, Evans JR (2009) Light and CO_2 do not affect the mesophyll conductance to CO_2 diffusion in wheat leaves. J Exp Bot 60:2291–2301

Tazoe Y, von Caemmerer S, Estavillo GM, Evans JR (2011) Using tunable diode laser spectroscopy to measure carbon isotope discrimination and mesophyll conductance to CO_2 diffusion dynamically at different CO_2 concentrations. Plant Cell Environ 34:580–591

Tcherkez G, Limami AN (2019) Net photosynthetic CO_2 assimilation: more than just CO_2 and O_2 reduction cycles. New Phytol 223:520–529

Tcherkez G, Gauthier P, Buckley TN et al (2017) Leaf day respiration: low CO_2 flux but high significance for metabolism and carbon balance. New Phytol 216:986–1001

Terashima I, Hanba YT, Tholen D, Niinemets Ü (2011) Leaf functional anatomy in relation to photosynthesis. Plant Physiol 155:108–116

Théroux-Rancourt G, Gilbert ME (2017) The light response of mesophyll conductance is controlled by structure across leaf profiles. Plant Cell Environ 40:726–740

Tholen D, Ethier G, Genty B, Pepin S, Zhu X-G (2012) Variable mesophyll conductance revisited: theoretical background and experimental implications. Plant Cell Environ 35:2087–2103

Tomas M, Flexas J, Copolovici L, Galmes J, Hallik L, Medrano H, Ribas-Carbo M, Tosens T, Vislap V, Niinemets Ü (2013) Importance of leaf anatomy in determining mesophyll diffusion conductance to CO_2 across species: quantitative limitations and scaling up by models. J Exp Bot 64:2269–2281

Tosens T, Niinemets Ü, Vislap V, Eichelmann H, Castro Diez P (2012a) Developmental changes in mesophyll diffusion conductance and photosynthetic capacity under different light and water availabilities in *Populus tremula*: how structure constrains function. Plant Cell Environ 35:839–856

Tosens T, Niinemets Ü, Westoby M, Wright IJ (2012b) Anatomical basis of variation in mesophyll resistance in eastern Australian sclerophylls: news of a long and winding path. J Exp Bot 63:5105–5119

Ubierna N, Cernusak LA, Holloway-Phillips M, Busch FA, Cousins AB, Farquhar GD (2019) Critical review: incorporating the arrangement of mitochondria and chloroplasts into models of

photosynthesis and carbon isotope discrimination. Photosynth Res 141:5–31

van der Putten PEL, Yin X, Struik PC (2018) Calibration matters: on the procedure of using the chlorophyll fluorescence method to estimate mesophyll conductance. J Plant Physiol 220:167–172

von Caemmerer S (2000) Biochemical models of leaf photosynthesis, vol 2. CSIRO Publishing, Collingwood

von Caemmerer S (2013) Steady-state models of photosynthesis. Plant Cell Environ 36:1617–1630

von Caemmerer S, Evans JR (1991) Determination of the average partial pressure of CO_2 in chloroplasts from leaves of several C_3 plants. Aust J Plant Physiol 18:287–305

von Caemmerer S, Evans JR, Hudson GS, Andrews TJ (1994) The kinetics of ribulose-1,5-bisphosphate carboxylase/oxygenase in vivo inferred from measurements of photosynthesis in leaves of transgenic tobacco. Planta 195:88–97

Vrábl D, Vašková M, Hronková M, Flexas J, Šantrůček J (2009) Mesophyll conductance to CO_2 transport estimated by two independent methods: effect of variable CO_2 concentration and abscisic acid. J Exp Bot 60:2315–2323

Warren CR, Dreyer E (2006) Temperature response of photosynthesis and internal conductance to CO_2: results from two independent approaches. J Exp Bot 57:3057–3067

Yamori W, Noguchi K, Hanba YT, Terashima I (2006) Effects of internal conductance on the temperature dependence of the photosynthetic rate in spinach leaves from contrasting growth temperatures. Plant Cell Physiol 47:1069–1080

Yin X, Struik PC (2009) Theoretical reconsiderations when estimating the mesophyll conductance to CO_2 diffusion in leaves of C_3 plants by analysis of combined gas exchange and chlorophyll fluorescence measurements. Plant Cell Environ 32:1513–1524 **(corrigendum in 33:1595)**

Yin X, Struik PC (2017) Simple generalisation of a mesophyll resistance model for various intracellular arrangements of chloroplasts and mitochondria in C_3 leaves. Photosynth Res 132:211–220

Yin X, Struik PC, Romero P, Harbinson J, Evers JB, van der Putten PEL, Vos J (2009) Using combined measurements of gas exchange and chlorophyll fluorescence to estimate parameters of a biochemical C_3 photosynthesis model: a critical appraisal and a new integrated approach applied to leaves in a wheat (*Triticum aestivum*) canopy. Plant Cell Environ 32:448–464

Yin X, Sun Z, Struik PC, Gu J (2011) Evaluating a new method to estimate the rate of leaf respiration in the light by analysis of combined gas exchange and chlorophyll fluorescence measurements. J Exp Bot 62:3489–3499